

Electronic Supporting Information (ESI)

COMMUNICATION

A polynuclear Cu(II) complex for real time monitoring of mitochondrial Cytochrome C release during cellular apoptosis

Received 00th January 20xx,
Accepted 00th January 20xx

DOI: 10.1039/x0xx00000x

Somnath Khanra,^a Sabyasachi Ta,^a Ankush Paladhi,^b Milan Ghosh,^a Subhasis Ghosh,^{a,b} Sumit Kumar Hira,^{*b} Partha Partim Manna,^{*c} Paula Brandão,^d Vítor Félix^{*d} and Debasis Das^{*ac}

Experimental

Materials, reagent and cells

All experiments have been carried out in aerobic conditions. High-purity HEPES buffer, 2-hydroxybenzoic acid, 2-hydroxy-benzaldehyde, hydrazine (NH₂NH₂) and thionyl chloride (SOCl₂) are purchased from Sigma Aldrich, USA. Cu(NO₃)₂·6H₂O are of reagent grade and purchased from Merck (India). Solvents used are of spectroscopic grade. Other chemicals are of analytical reagent grade and used without further purification except when specified. Mili-Q Milipore 18.2 MΩ.cm water is used whenever required. DL (murine lymphoma) cells MCF-7 (human breast carcinoma) and NIH/3T3 (primary mouse embryonic fibroblast cells) cells have been grown in complete RPMI 1640 and DMEM medium at 37°C in a humidified atmosphere containing 5% CO₂. MitoTracker Red CMXRos is purchased from Invitrogen USA.

Physical measurements

Elemental PerkinElmer 2400 series II CHN analyzer have been used for elemental analysis. FTIR spectra are recorded on a Shimadzu FTIR (model IR Prestige

21 CE) spectrometer. The UV-Vis. spectra (800–200 nm) are collected with Shimadzu Multi Spec 2450 spectrophotometer. Systronics digital pH meter (model 335) and HCl/ NaOH (50 μM) are used for measurement of pH. The cell path length for recording spectra is 1 cm. Electrospray ionization mass spectra (ESI-MS⁺) are recorded with a Thermo Fisher Scientific Exactive Plus mass spectrometer at a flow rate of 5 μL min⁻¹ in spectroscopic grade methanol having compound concentration, 10⁻⁶ M. ¹HNMR spectra are collected from Bruker 400 MHz spectrometer using DMSO-*d*₆ as solvent, the chemical shift is represented in ppm with residual solvent peak as an internal reference. Multiplicity is indicated as follows: s (singlet), d (doublet), t (triplet), q (quartet), m (multiplet). Coupling constants (J, s) are reported in Hertz (Hz). Cyclicvoltammetric (CV) studies have been performed in dry acetonitrile using CHI620D potentiometer having three-electrode configuration: a platinum disk working electrode, a platinum wire auxiliary electrode and a calomel reference electrode, extensively purged with N₂ prior to measurements using 0.1M TBAP as supporting electrolyte. All potentials are measured at a scan rate of 100 mV s⁻¹ at room temperature.

The single crystal X-ray diffraction data are collected on a Bruker X8 APEXII CCD diffractometer at 150(2) K, using graphite-monochromatic Mo-K_α radiation (0.71073 Å). Significant crystal parameters and refinement data are summarized in **Table S2, ESI**.

^a Department of Chemistry, The University of Burdwan, Burdwan, 713104, W.B., India

^b Cellular Immunology laboratory, Department of Zoology, The University of Burdwan, Burdwan, 713104, W.B., India

^c Immunobiology laboratory, Department of Zoology, Institute of Science, Banaras Hindu University, Varanasi-221005, India

^d CICECO – Aveiro Institute of Materials, Department of Chemistry, University of Aveiro, 3810-193 – Aveiro, Portugal

†Correspondence: ddas100in@yahoo.com (D. Das), sumit.hira2008@gmail.com (SKH), pp_manna@yahoo.com (PPM) and viktor.felix@ua.pt (V Félix)

Data are processed and corrected for Lorentz and polarization effects. Using the Olex2 graphical interface,¹ the structure was solved by intrinsic phasing with ShelXT² and refined by full matrix least square ShelXL.³ All non-hydrogen atoms are anisotropic thermal parameters. Hydrogen atoms are included in the structure factor calculation in geometrically idealized positions with isotropic thermal displacements depending on the parent atom, using a riding model. Molecular diagrams were drawn with Mercury software.⁴

Synthesis

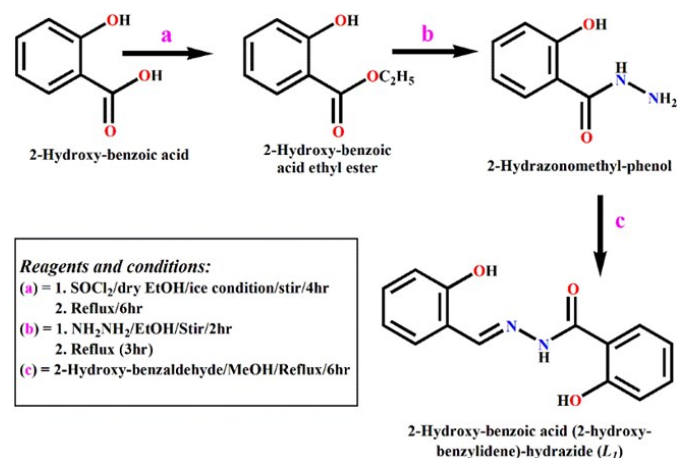
2-Hydrazonomethyl-phenol (**L**)

To an ethanol solution of 2-hydroxy-benzoic acid, few drops of SOCl_2 were added under stirring condition for 4h in ice-cold condition (**Scheme S1**, **ESI**). The reaction mixture is then refluxed for 6h to corresponding ethyl ester. The resulting ester is treated with hydrazine leading to 2-hydrazonomethyl-phenol (**L**) in 52% yield. Anal. found, C, 54.75; H, 5.61 and N, 16.96; calcd., C, 55.26; H, 5.30 and N, 18.41. The ESI-MS (m/z): $[\text{M}+\text{MeOH}+\text{Na}]^+$, 206.48. (**Figure S1a**, **ESI**). ¹HNMR (**Figure S1b**, **ESI**), 400 MHz, $\text{DMSO}-d_6$, TMS, δ (ppm): a. 11.74 (1H, s), b. 7.734 (1H, s), c. 4.11 (2H, t, $J = 6.8$), 7.419 (1H, m), 7.325 (1H, m), 7.00 (1H, m), 6.86 (1H, m). ¹³CNMR (**Figure S1c**, **ESI**): 167.95, 159.60, 133.48, 127.19, 118.74, 117.36, and 114.48. FTIR (KBr, cm^{-1}): 3000, ν (N-H); 2850 ν (C-H of CH_3); 1581 ν (C=O) (**Figure S1d**, **ESI**)

2-Hydroxy-benzoic acid (2-hydroxy-benzylidene)-hydrazide (**L₁**)

The mixture of **L** (152 mg, 1 mmol) and 2-hydroxybenzaldehyde (122 mg, 1 mmol) in methanol was refluxed for 6h (**Scheme 1**, **ESI**) to yield 73% **L₁**. Anal. found, C, 64.08; H, 4.69 and N, 10.49; calcd., C, 65.02; H, 4.72 and N, 10.93. The ESI-MS (m/z): $[\text{M}]^+$, 255.23 (**Figure S2a**, **ESI**). ¹H NMR (CDCl_3 , 400 MHz, δ ppm, reference, δ 2.5 ppm) (**Figure S2b**, **ESI**): 12.038 (1H, s) 11.783 (1H, s), 11.220 (1H, s) 8.674 (1H, s), 7.895-7.875 (1H, d, 8.0 $J = 8.0$ Hz), 7.573-7.550 (1H, q) 7.471-7.429 (1H, m), 7.330-7.291 (1H, q), 6.998-6.907 (4H, m). FTIR (KBr, cm^{-1}): 3444.17, ν (N-H); 3184.39, ν (O-H); 3053.80, ν (C-H, aromatic);

2916.04, ν (C-H, aldehyde); 1616.77, ν (C=O, stretch); 1540.06, ν (C=N); 1378.37, ν (C-N); 1148.21, ν (N-N) (**Figure S2c**, **ESI**)



Scheme 1 Synthesis of **L** and **L₁**.

Polymeric Cu(II) complex (**M1**)

Methanol solution of $\text{Cu}(\text{NO}_3)_2 \cdot 6\text{H}_2\text{O}$ (295 mg, 1 mmol, 5 mL) was added to the solution of **L₁** (256 mg, 1 mmol, 5 mL) in methanol under stirring condition for 2h. Slow evaporation of solvent resulted dark green crystals, suitable for X-ray diffraction analysis in 61% yield. The ESI-MS (m/z), $[\text{M}+\text{H}]^+$, 318.07 corresponds to the asymmetric unit. (**Figure S3a**, **ESI**). FTIR (KBr, cm^{-1}): 3453.90, ν (N-H); 3038.96, ν (C-H, aromatic); 1625.02, ν (C=O, stretch); 1516.96, ν (C=N); 1363.52, ν (C-N); 1294.22, ν (C=O, stretch); 1148.21, ν (N-N) (**Figure S3b**, **ESI**).

General method of UV-Vis and fluorescence titration

Path length of the cells used for absorption and emission studies is 1 cm. For UV-Vis and fluorescence titrations, stock solution of **M1** is prepared (20 μM) in EtOH /water, 1/1, v/v, 0.1 M HEPES buffer, pH 7.4. Working solutions of **M1**, and **Cyt C** are prepared from their respective stock solutions. Fluorescence measurements have been performed using 5 nm x 5 nm slit width.

Determination of binding constant

The binding constants of compound **M1** for different analyte are determined using the following Benesi-Hildebrand equation.⁵

$$\frac{F_{max} - F_{min}}{F_x - F_{min}} = 1 + \frac{1}{K[C]^n}$$

Where F_{min} , F_x , and F_{max} are the emission intensities of the compound **M1** in absence of analyte, at an intermediate analyte concentration, and at a concentration of complete interaction with analyte respectively. K is the binding constant, C is the concentration of analyte and n is the number of analyte bound per probe molecule (assuming, $n = 1$). The value of K are obtained from the slopes of different plot for different analyte.

Calculation of detection limit

The detection limit (**DL**) is determined from the following equation.⁶

$$DL = \frac{3\sigma}{S}$$

σ is the standard deviation of the blank solution, S is the slope of the calibration curve.

For the determination of standard deviation the emission intensity of **M1** without any analyte was measured by 10 times.

Induction of cell death and detection of Cyt C by fluorescence microscope

DL or MCF cells were plated in a 48 well cell culture plate and incubated with the solution containing 50 nM **M1** in the serum free RPMI 1640 medium at 37°C for 1h for cellular uptake of the **M1**. Following incubation, the cells were washed three times with cold PBS, and were further incubated in fresh RPMI 1640 medium containing Staurosporine (StS) of a given concentration for additional 1.5 h at 37°C. Each well was washed twice with cold PBS before imaging. For the time-dependent fluorescence imaging of Cyt C translocation in apoptotic cells were performed in DL cells, plated on in a 48 well plate and incubated with 10 $\mu\text{g mL}^{-1}$ **M1** in culture medium for another 1 h. The cells were then treated with 1 μM StS. The fluorescence images were taken immediately after the addition of StS at regular time interval. The real-time fluorescence images were

collected using DMI8 Fluorescence microscope (Leica Microsystem, GmbH) fitted with COOLED light source. Images were captured using LAS-X software and were analysed by Image-Pro Plus image processing software. Localization of the Mitochondrial Cytochrome C in living cells and apoptotic cell by **M1** was performed using the same protocol except an additional step of treatment with 20 nM Mitochondria tracer (Mito@trackerRed) for 20 min following StS exposure before imaging.

Electronic Supporting Information (ESI)

COMMUNICATION

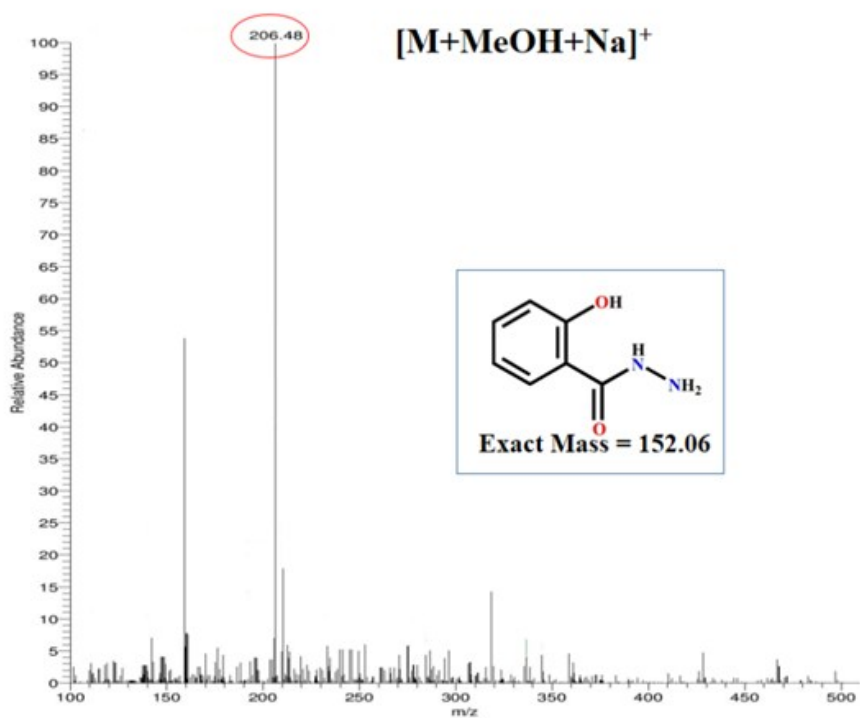
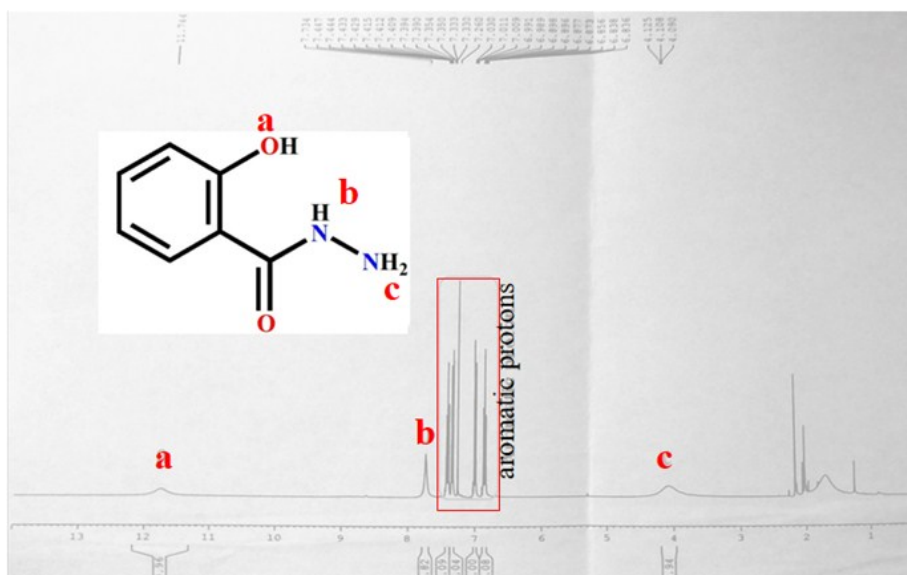


Figure S 1a QTOF mass spectrum of L.

Figure S 1b 1H NMR spectrum of L

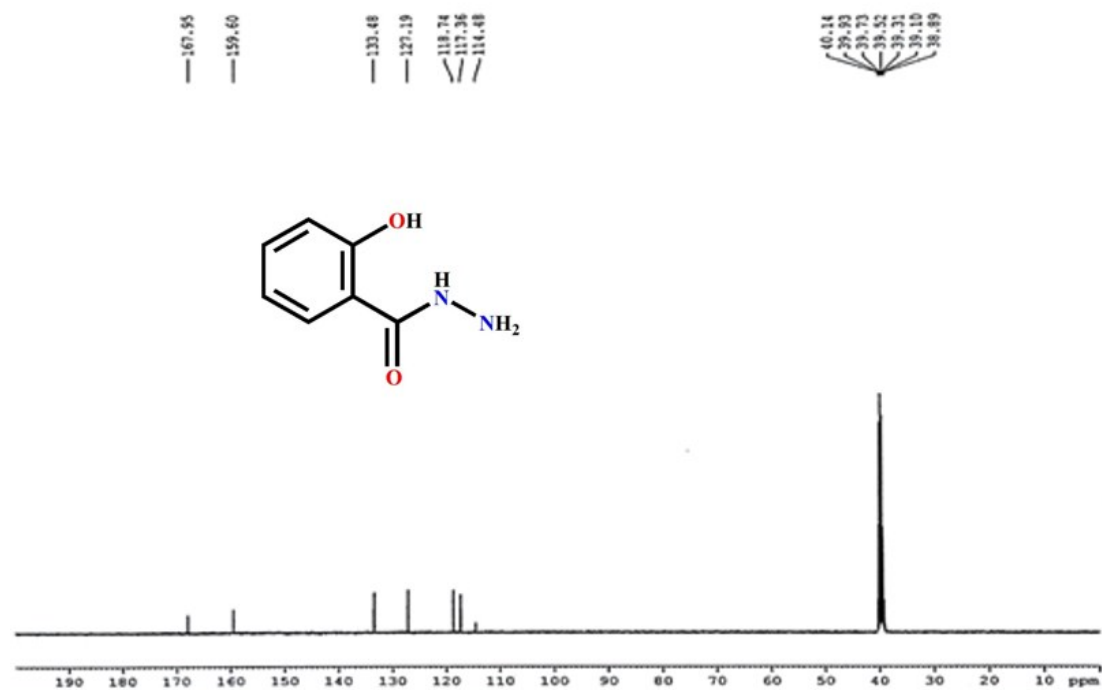
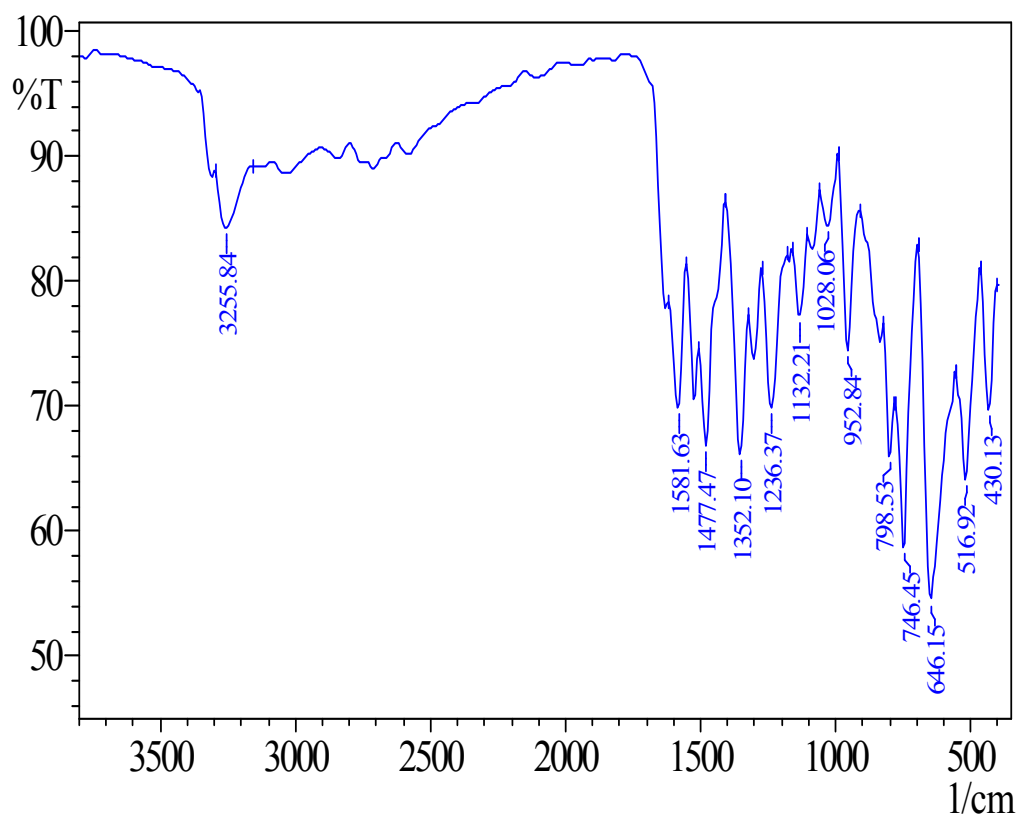
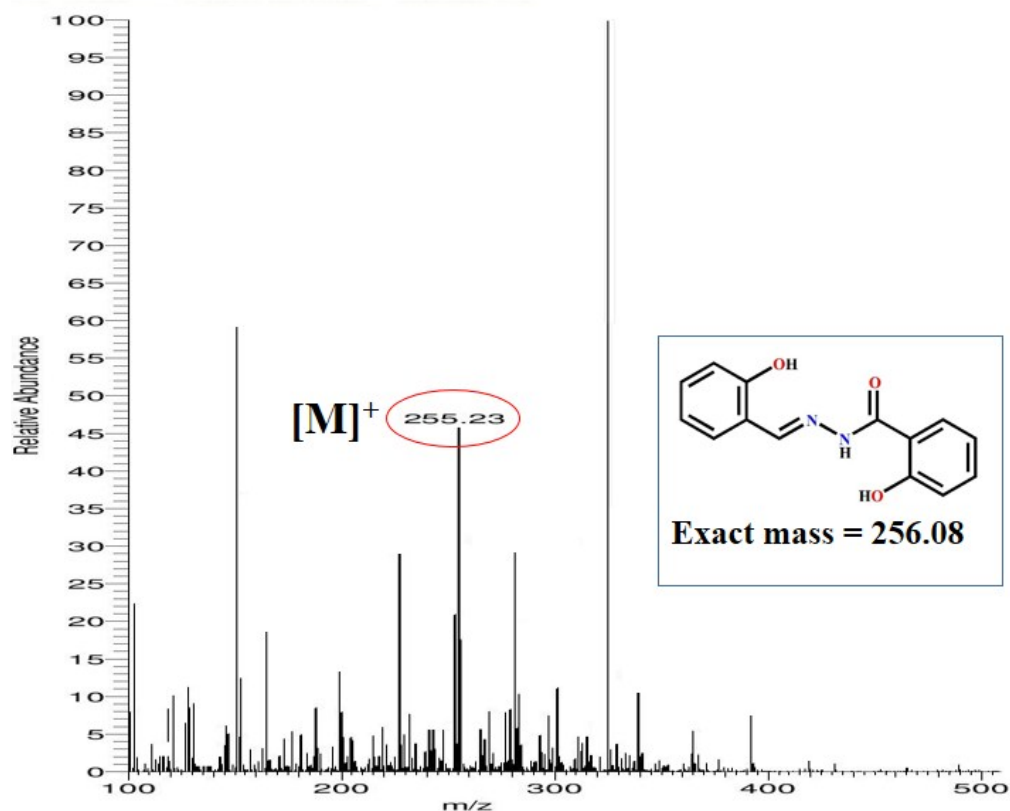
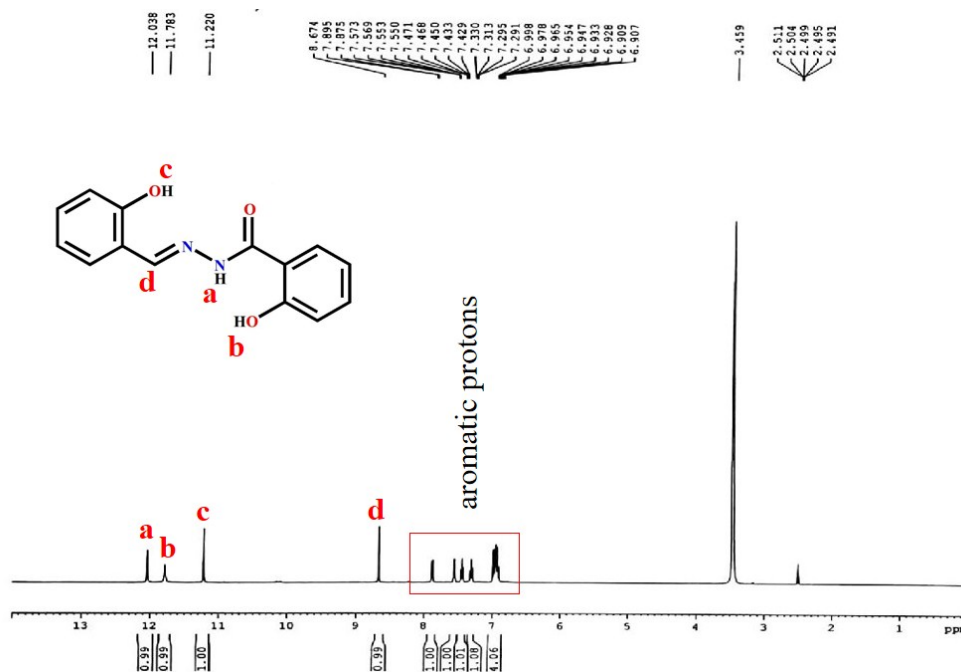
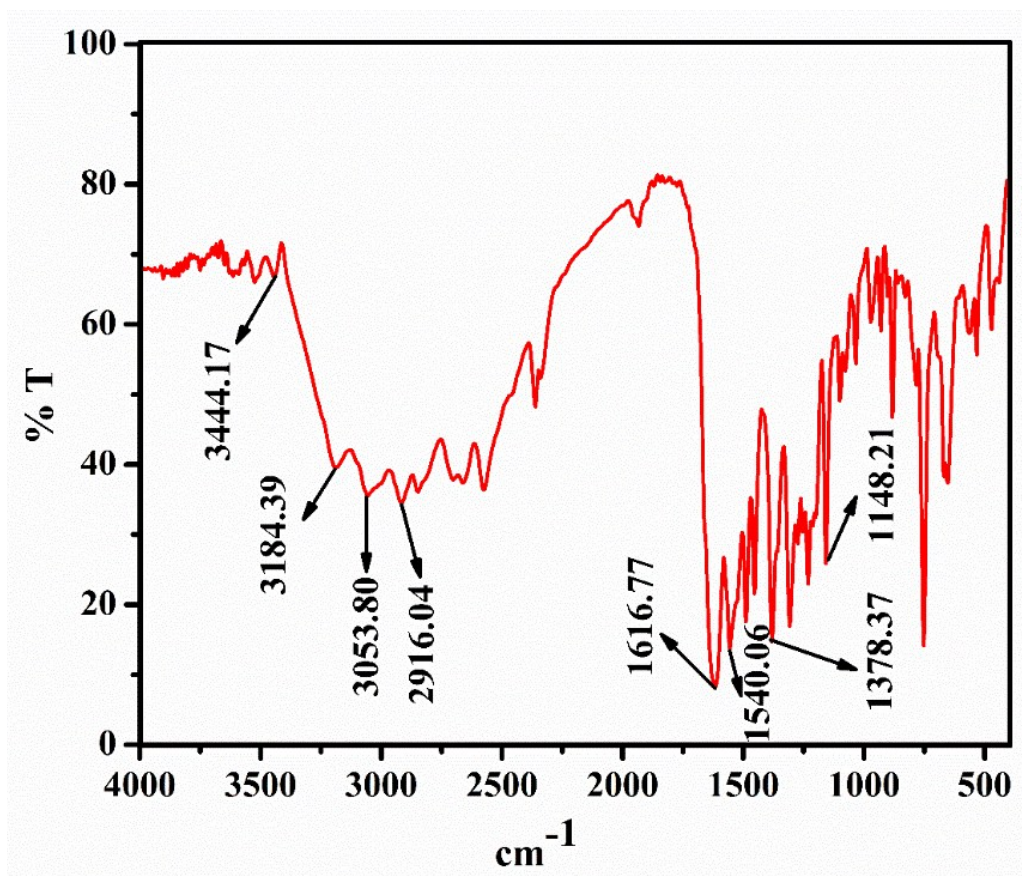
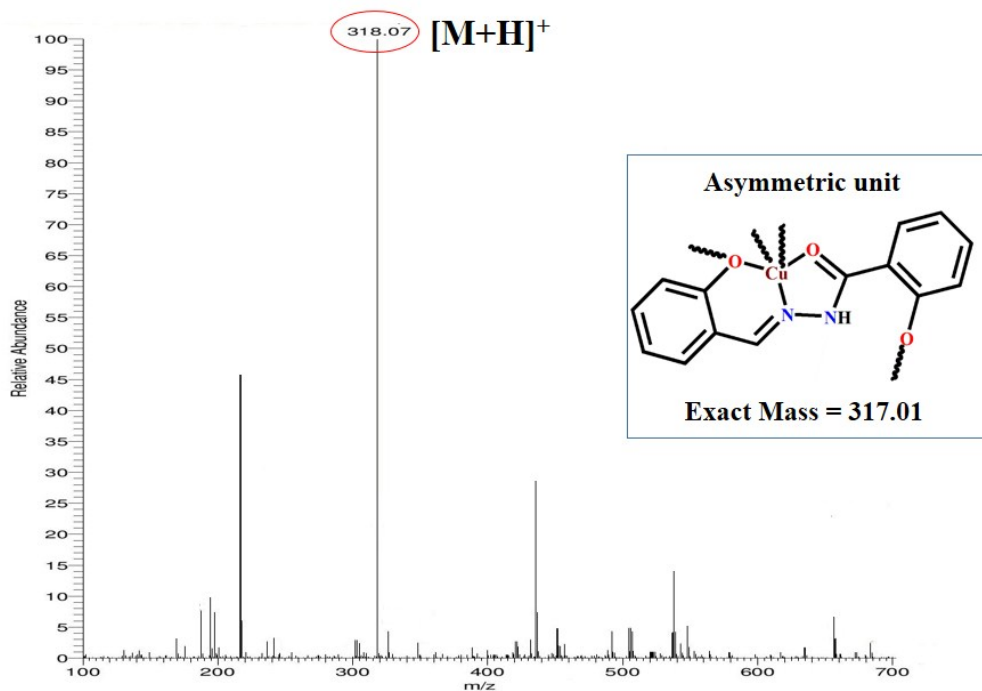
Figure S 1c ^{13}C NMR spectrum of L

Figure S 1d FTIR spectrum of L.

Figure S 2a QTOF mass spectrum of L_1 .Figure S2b 1H NMR spectrum of L_1 .

Figure S2c FTIR spectrum of L_1 .Figure S3a QTOF mass spectrum of M_1 .

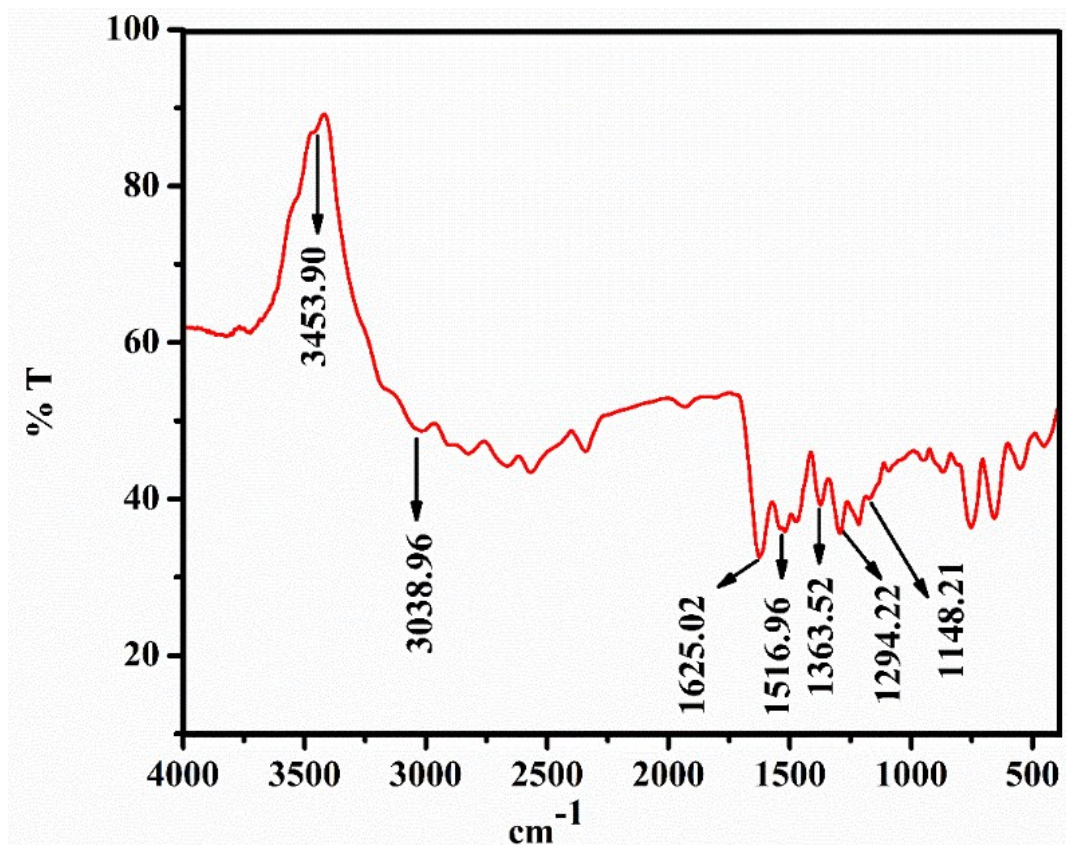


Figure S3b FTIR spectrum of M1.

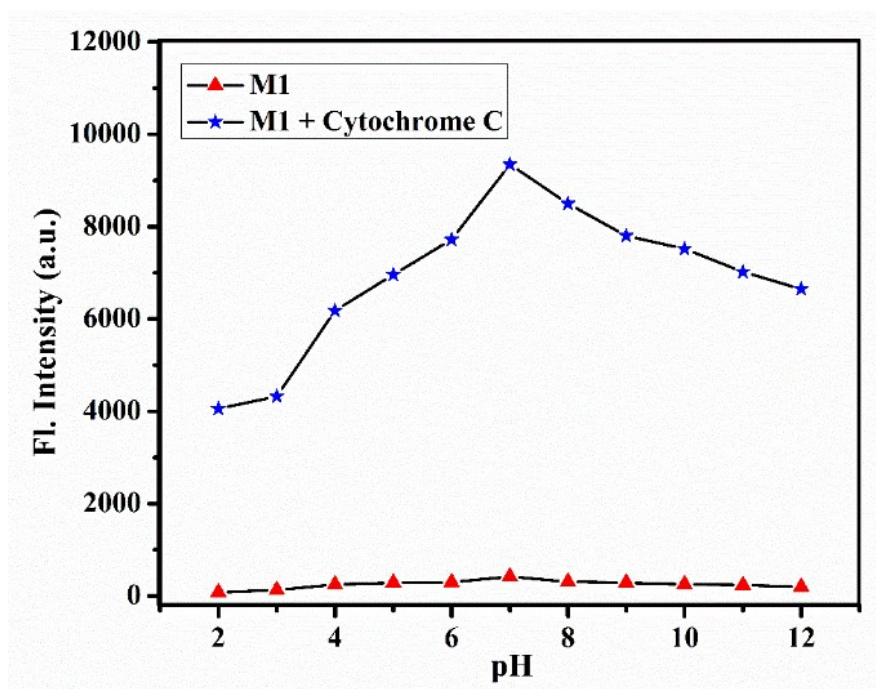


Figure S4 Effect of pH on the emission intensities of M1, ($\lambda_{\text{ex}} = 385 \text{ nm}$, $\lambda_{\text{em}} = 481 \text{ nm}$) in presence and absence of Cyt C.

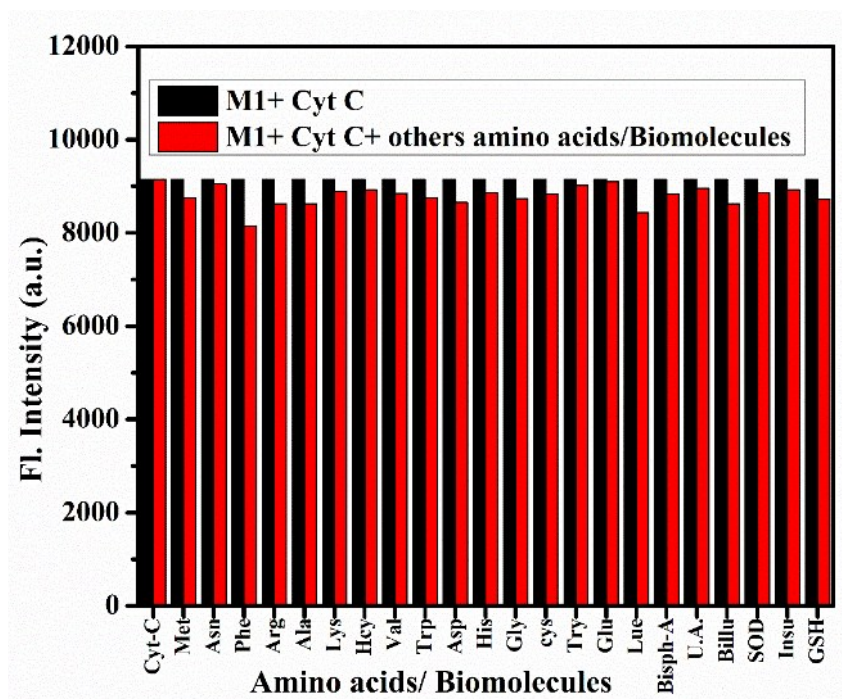


Figure S5 Interference plot for **Cyt C** determination using **M1** by fluorescence ($\lambda_{\text{ex}} = 385 \text{ nm}$, $\lambda_{\text{em}} = 481 \text{ nm}$).

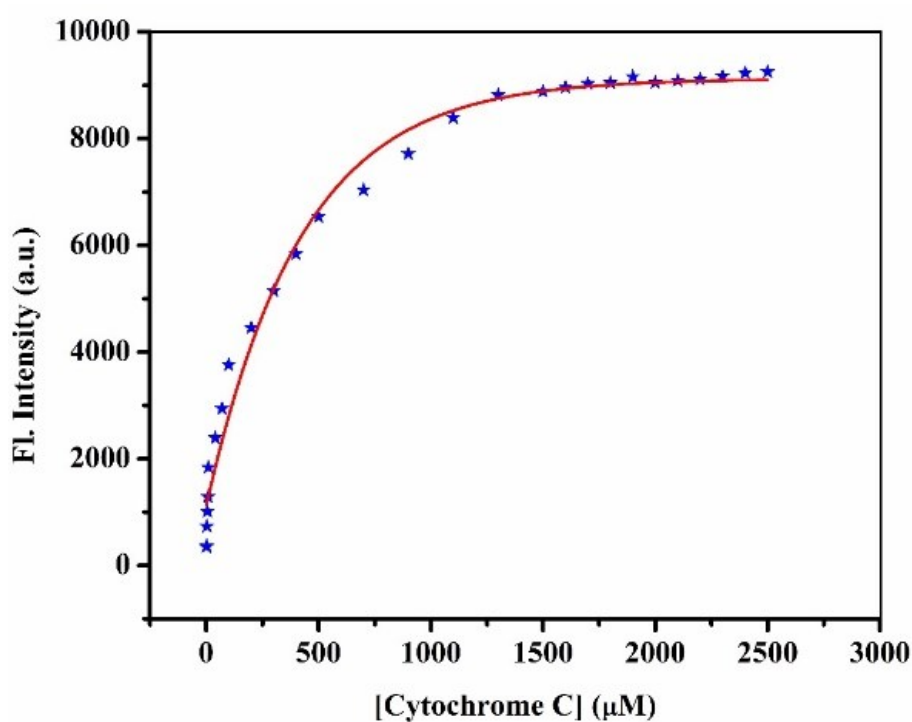


Figure S6 Plot of emission intensities of **M1** ($20 \mu\text{M}$, $\lambda_{\text{ex}} = 385 \text{ nm}$, $\lambda_{\text{em}} = 481 \text{ nm}$) as a function of added **Cyt C** ($1.0\text{-}2500 \mu\text{M}$).

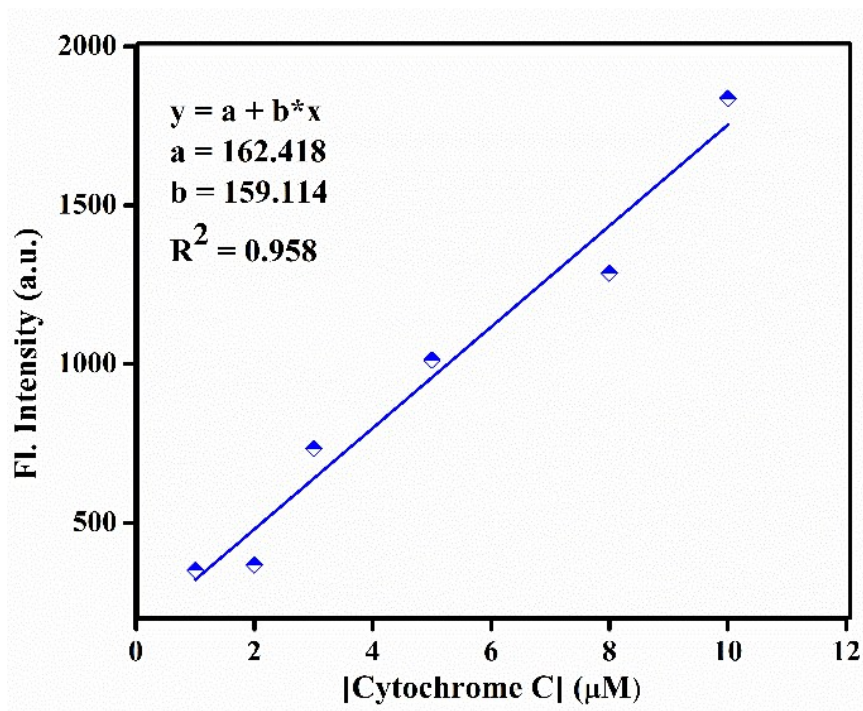


Figure S7 Determination of detection limit based on change in the ratio (emission intensity at $\lambda_{\text{em}} = 481$ nm, $\lambda_{\text{ex}} = 385$ nm,) of **M1** (20 μM) with **Cyt C**, linear portion of Figure S6.

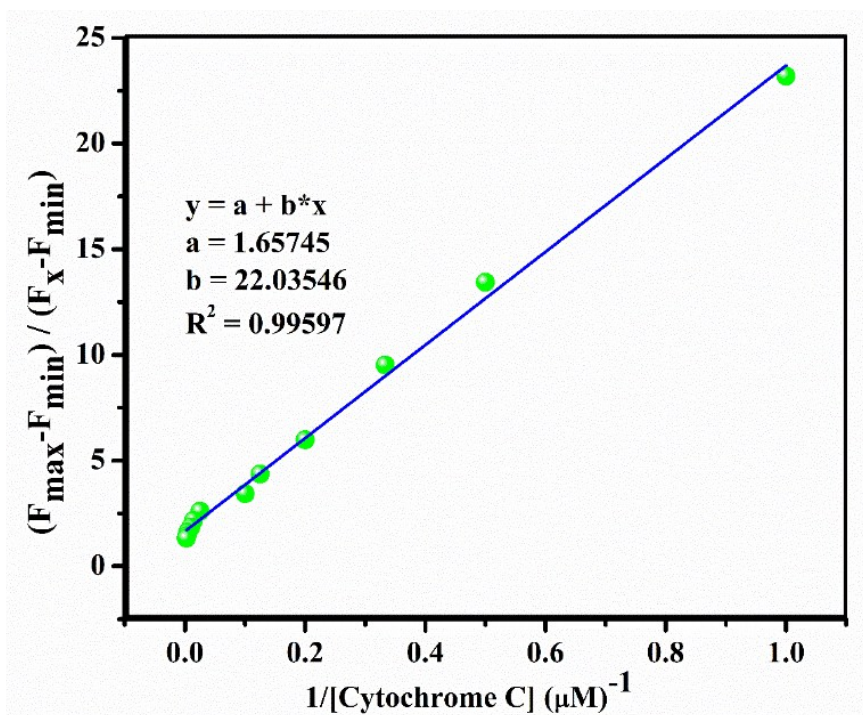


Figure S8 Benesi-Hildebrand plot for determination of association constant of **M1** with **Cyt C** (linear portion only), $\lambda_{\text{ex}} = 385$ nm, $\lambda_{\text{em}} = 481$ nm

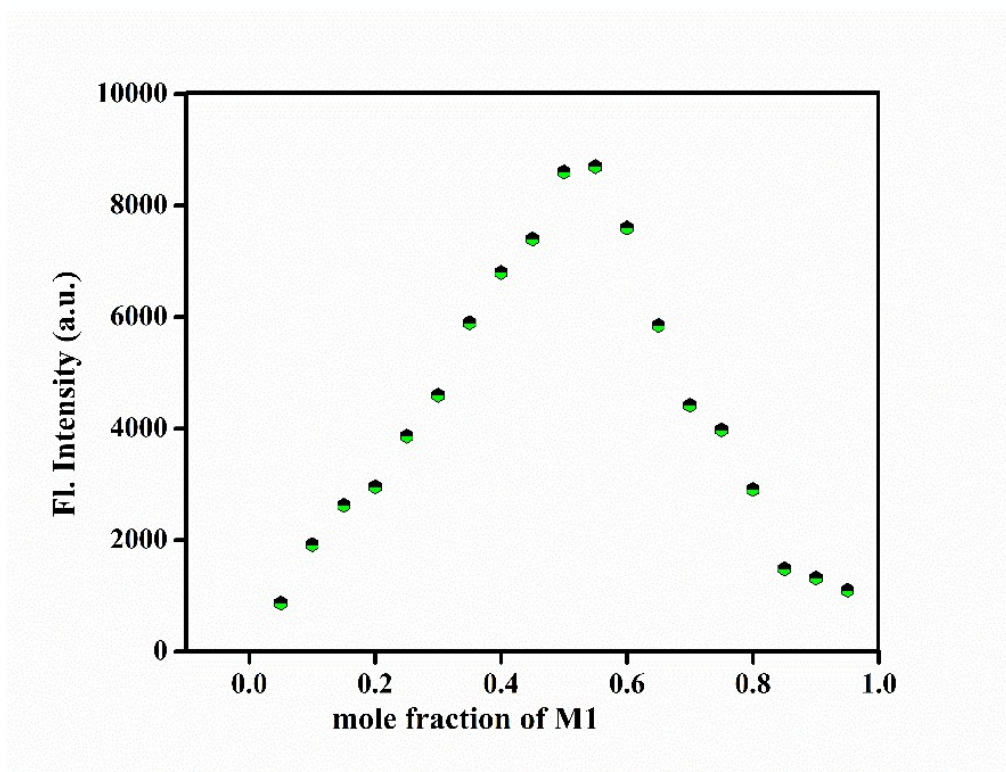


Figure S9 Jobs plot for stoichiometry determination ($\lambda_{\text{ex}} = 385 \text{ nm}$, $\lambda_{\text{em}} = 481 \text{ nm}$)

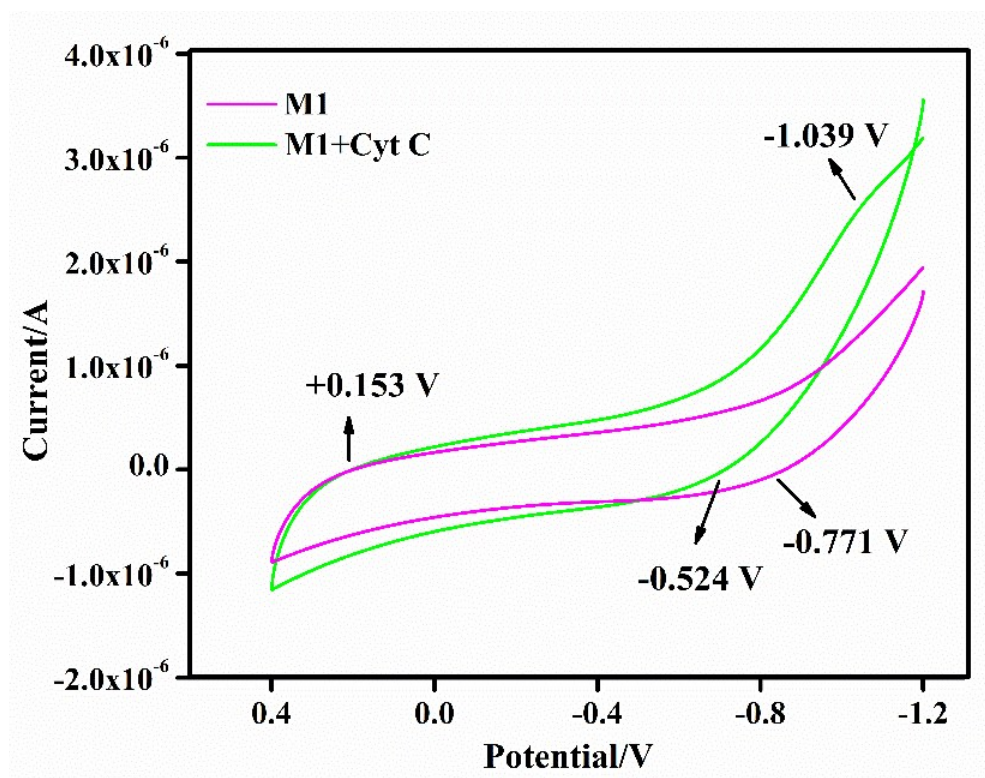


Figure S10 Cyclic voltammograms of M1 and M1-Cyt C.

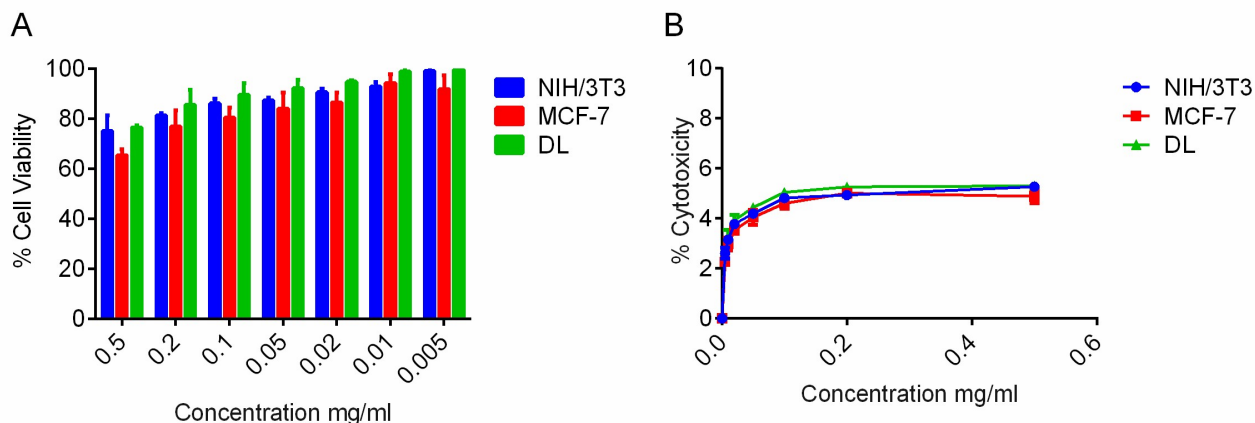


Figure S11 Proliferation of NIH/3T3, MCF-7 & DL cells in presence of M1 was studied following MTT assay (A). Line Graphs show cytotoxicity of NIH/3T3, MCF-7 & DL cells following treatment with M1 for 18h. LDH release assay was performed. Data presented as mean \pm SD, n = 4.

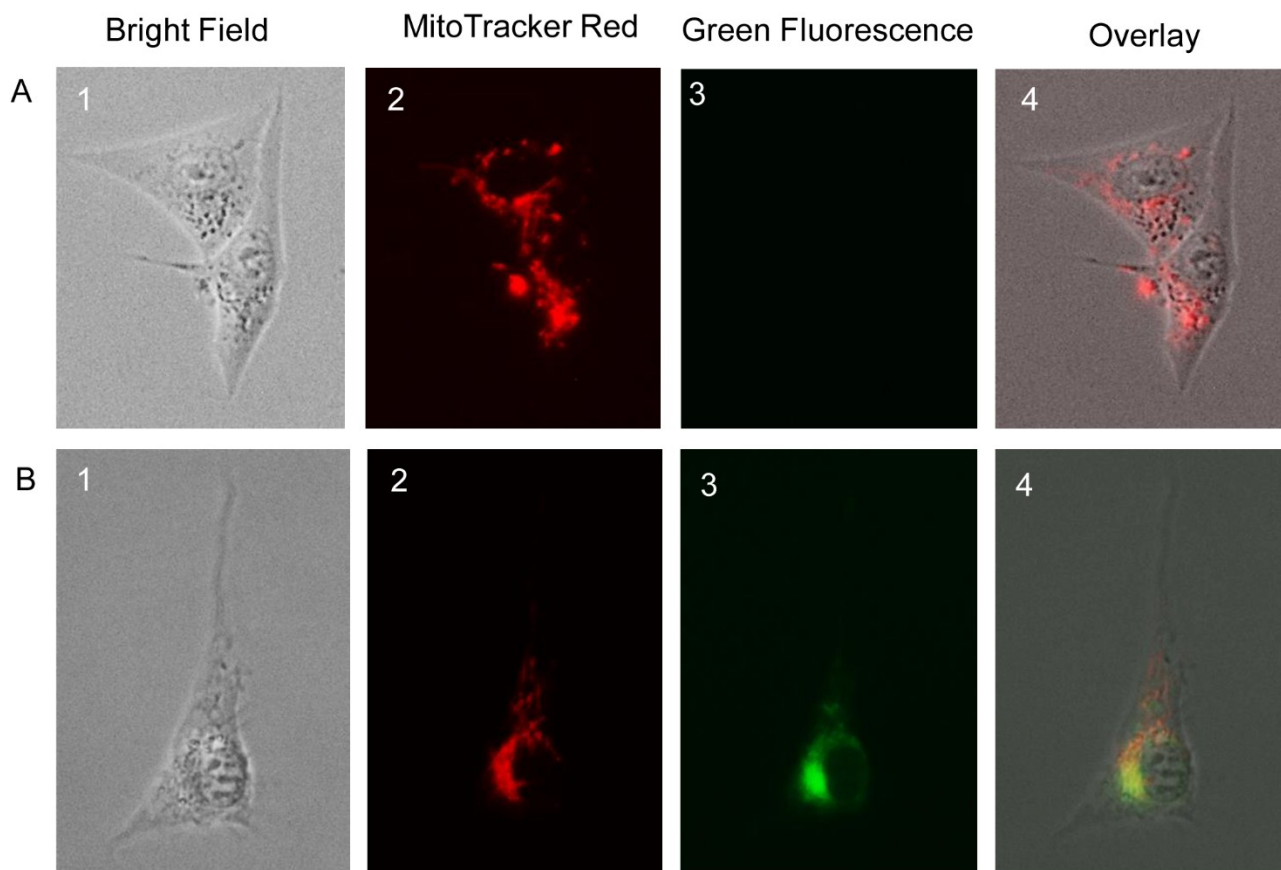


Figure S12 Mitochondrial localization of Cyt C by fluorescence imaging in MCF-7 cells using $10 \mu\text{g mL}^{-1}$ M1 (A) no treatment (B) $1 \mu\text{M}$ StS treated. (Magnification 1000 \times)

Table S1 Selected bond lengths (Å) and bond angles (°) of **M1**

Cu...Cu*	2.9991(10)		
Cu-O(17)	1.944(3)	Cu-O(17) ¹	1.974(3)
Cu-O(18)	1.925(3)	Cu-N(8)	1.916(4)
Cu-O(17)-Cu*	99.91(13)	N(8)-Cu-O(17)*	168.52(15)
O(18)-Cu-O(17)	174.83(13)	O(18)-Cu-O(17)*	105.05(13)
N(8)-Cu-O(17)	93.47(14)	N(8)-Cu-O(18)	81.56(14)

*means the symmetry operator: -x,1-y,1-z

Table S2 Summary of crystallographic data and refinement details of **M1**

Empirical formula	C ₁₄ H ₁₀ N ₂ O ₃ Cu
Formula weight	317.78
Crystal system	Monoclinic
Space group	<i>P</i> 2 ₁ / <i>n</i>
<i>a</i> /Å	6.4066(6)
<i>b</i> /Å	18.6435(16)
<i>c</i> /Å	9.8389(10)
β /°	96.696(3)
Volume/Å ³	1167.16(19)
<i>Z</i>	4
ρ_{calc} g/cm ³	1.808
μ /mm ⁻¹	1.879
<i>F</i> (000)	644.0
2 θ for data collection/°	4.37 to 54.242
Index ranges	-8 ≤ <i>h</i> ≤ 8, -23 ≤ <i>k</i> ≤ 23, -12 ≤ <i>l</i> ≤ 12
Reflections collected	20090
Independent reflections	2477 [<i>R</i> _{int} = 0.0674, <i>R</i> _{sigma} = 0.0422]
Data/restraints/parameters	2477/0/181
Goodness-of-fit on <i>F</i> ²	1.134
Final <i>R</i> indexes [<i>I</i> ≥ 2 σ (<i>I</i>)]	<i>R</i> ₁ = 0.0531, <i>wR</i> ₂ = 0.1377
Final <i>R</i> indexes [all data]	<i>R</i> ₁ = 0.0711, <i>wR</i> ₂ = 0.1461
Largest diff. peak/hole /eÅ ⁻³	1.23/-0.76

References

1. O. V. Dolomanov, L. J. Bourhis, R. J. Gildea, J. A. K. Howard and H. Puschmann, *J Appl. Crystallogr.*, 2009, **42**, 339-341.
2. G. Sheldrick, *Acta Crystallograph. A*, 2015, **71**, 3-8.
3. G. Sheldrick, *Acta Crystallograph. C*, 2015, **71**, 3-8.
4. C. F. Macrae, I. J. Bruno, J. A. Chisholm, P. R. Edgington, P. McCabe, E. Pidcock, L. Rodriguez-Monge, R. Taylor, J. van de Streek and P. A. Wood, *Journal of Applied Crystallography*, 2008, **41**, 466-470.
5. H. A. Benesi and J. H. Hildebrand, *J. Am. Chem. Soc.*, 1949, **71**, 2703.
6. M. Zhu, M. Yuan, X. Liu, J. Xu, J. Lv, C. Huang, H. Liu, Y. Li, S. Wang, D. Zhu, *Org. Lett.*, 2008, **10**, 1481.